MEASURING THE MIXING EFFICIENCY IN A SIMPLE MODEL OF STIRRING:SOME ANALYTICAL RESULTS AND A QUANTITATIVE STUDY VIA FREQUENCY MAP ANALYSIS

TIMOTEO CARLETTI AND ALESSANDRO MARGHERI

Abstract. We prove the existence of invariant curves for a T–periodic Hamiltonian system which models a fluid stirring in a cylindrical tank, when T is small and the assigned stirring protocol is piecewise constant. Furthermore, using the Numerical Analysis of the Fundamental Frequency of Laskar, we investigate numerically the break down of invariant curves as T increases and we give a quantitative estimate of the efficiency of the mixing.

1. Introduction

In [1] it is studied a simplified model of the stirring of an ideal fluid in a cylindrical tank by an agitator. A Lagrangian representation is considered for the motion, which is assumed to be completely two dimensional. The tank thus degenerates to its boundary circle, which has radius R. The agitator is modelled as a point vortex of strength Γ and its position inside the boundary circle as a function of time, denoted by $z(t)$, is a prescribed T–periodic function called *stirring protocol*. Introducing the complex coordinate $\zeta = x + iy$, the motion of the fluid is governed by the following nonautonomous T–periodic Hamiltonian system

$$\dot{\bar{\zeta}} = \frac{\Gamma}{2\pi i}\frac{|z(t)|^2 - R^2}{(\zeta - z(t))(\zeta\overline{z(t)} - R^2)}\,, \tag{1}$$

whose corresponding Hamilton function is given by

$$H(t,\zeta) = \frac{\Gamma}{2\pi}\ln\left|\frac{\zeta - z(t)}{\overline{z(t)}\zeta - R^2}\right|\,. \tag{2}$$

System (1) is defined on the set $\{(t,\zeta) \in \mathbb{R}\times\mathbb{C} : \zeta \neq z(t), \zeta \neq \frac{R^2}{\overline{z(t)}}\}$ and it is considered for ζ belonging to the invariant disk $D_R = \{\zeta \in$

1991 *Mathematics Subject Classification.* PACS numbers: 05.45.Gg, 47.52.+j ,47.11.+j.

Key words and phrases. mixing, invariant curves, frequency map, averaging theory.

$\mathbb{C} : |\zeta| \leq R\}$. The following piecewise constant stirring protocol

$$z(t) = \begin{cases} +b & t \in \Big[nT, nT + T/2\Big) \\ -b & t \in \Big[nT + T/2, (n+1)T\Big) \quad n \in \mathbb{Z}\,, \end{cases} \tag{3}$$

with fixed $0 < b < R$, has been investigated in [1]. In this case the motion can be integrated over finite time, whereas the long time behavior of the model is studied by numerical experiments when $b = 1/2$ for different values of T. In [1], the objective of the author is to study which features control the onset of chaos and hence the efficiency of the mixing. For this aim, the regimes of regular and chaotic behavior are identified and a *qualitative* description (see [1] page 736 second paragraph) of the mixing efficiency of the model has been provided for several values of the parameters (b, T). It turns out that the regions of chaotic behavior consume a larger and larger portion of the phase space as T increases, disrupting the regular pattern observed when T is very small (see Figure 1). Quoting [1], '*...for small T the model [...] will look more and more like the two fixed agitator system; [...] Thus one would expect 'convergence' as $T \to 0$.* '

In Section 2 of this work we will show that averaging theory provides the appropriate framework to investigate the above statement. Loosely speaking, in such a setting we will be able to show that when $T \to 0$ the flow of system (1) with the stirring protocol (3) converges in the C^4 topology to the Hamiltonian flow corresponding to two fixed agitators. As a consequence, by using Moser's Small Twist Theorem ([13],[14],[7],[8]) we will prove that the regularity of the pattern observed in the numerical experiments for small T (see Figure 2 a), b) and c) page 733 of [1] and Figure 1 for $T = 0.05$) is due, at least in a suitable annular region inside D_R, to the presence of invariant curves. In fact, such curves are, as one readily realizes, an obstruction to the mixing of the fluid.

The result which we present with this respect is the following:

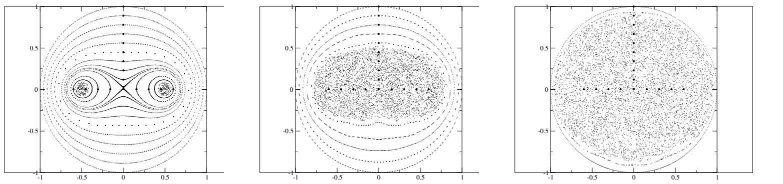

FIGURE 1. Different behaviors of the Poincaré map, with $b = 1/2$, $R = 1$ and $T = 0.05$ (left), $T = 0.5$ (middle) and $T = 1.5$ (right). Each plot is obtained following 10000 time units the same 18 initial data.

Theorem 1. *Let $z(t)$ be the stirring protocol (3) and let $T > 0$ be its period. Then, there exists an annular region A inside D_R such that the*

T–Poincaré map associated to system (1) has invariant curves in A for any sufficiently small T.

As T increases the invariant curves break down. In Section 3, we will study numerically this phenomenon by means of the *Numerical Analysis of the Fundamental Frequency, NAFF* of Laskar [10]. This allows us to extend our previous analytical result to cover larger T ranges, by showing numerical evidence that invariant curves persist close enough to the boundary of the invariant disk D_R for large values of T. Furthermore, we are able to give a *quantitative* description of the efficiency of the mixing in function of the parameters (b, T), by measuring, through NAFF, the portion of phase space filled by invariant curves.

Acknowledgements. Support from GRICES/CNR project is acknowledged. The second author would also thank support from FCT

2. Existence of invariant curves

In order to establish the existence of invariant curves for system (1) with the piecewise constant protocol (3) and small T, we will show that its T–Poincaré operator (i.e. its period map) satisfies the assumptions of the so called *Moser's Small Twist Theorem.*

Before outlining the strategy of our proof, it is worth to recall the statement of this important result.

Fixed $I_1 > I_0 > 0$, let us consider the annulus defined by $A = \{(\bar{\theta}, I) : \bar{\theta} \in \mathbb{S}^1 \,, I_0 \le I \le I_1\}$. Given a mapping $M : A \to \mathbb{R}^2$, we can find a lift to the universal cover $\mathcal{A} = \{(\theta, I) : \theta \in \mathbb{R} \,, I_0 \le I \le I_1\}$ of A, which we still denote by M.

Moser's Small Twist Theorem *Let α be a $C^4([I_0, I_1])$ function satisfying*

$$\alpha'(I) < 0 \quad \forall I \in [I_0, I_1] \,. \tag{4}$$

Then, there exists $\epsilon > 0$, depending on $I_1 - I_0$ and α, such that the map $M : A \mapsto \mathbb{R}^2$ has invariant curves if it satisfies the conditions below

a) *M has the intersection property, that is, for any Jordan curve γ homotopic to the circle $I = I_0$ in A, $M(\gamma) \cap \gamma \not\equiv \emptyset$;*
b) *the lift of M can be expressed in the form*

$$M(\theta, I) = (\theta + T\alpha(I) + T\phi_1(\theta, I, T), I + T\phi_2(\theta, I, T)) \,, \tag{5}$$

for some $T \in (0, 1)$ and $\phi_1, \phi_2 \in C^4(\mathcal{A})$ with $||\phi_1||_{C^4(\mathcal{A})} + ||\phi_2||_{C^4(\mathcal{A})} < \epsilon$.

This version of the theorem is presented in [14] and may be proved using the techniques developed in [7, 8].

In what follows, a map of the form $(\theta + T\alpha(I), I)$ with $\alpha'(I) \neq 0$, $I \in [I_0, I_1]$, will be referred to as *small twist map.*

The application of the previous theorem will be obtained performing the following steps. First, by using a classical construction from averaging theory, in Subsection 2.1 we will rewrite system (1) as a 1–periodic perturbation of the Hamiltonian averaged system, being T the small parameter. The averaged system corresponds to the two fixed agitator model. Then, exploiting the geometry of the phase space of the averaged system, we will construct explicitly the corresponding action variable on a suitable subset of D_R. As a consequence, we will be able to show that on an appropriate annulus inside D_R the 1–Poincaré map of the averaged system is a small twist map.

Next, the C^4 estimates needed to apply the Small Twist Theorem will be provided by a general result about the differentiability of a flow with respect to parameters, which we recall in Proposition 2 of Subsection 2.2.

Finally, in Subsection 2.3, we collect all these fact and complete the proof of Theorem 1.

2.1. **The averaged system.** In what follows, we identify $\mathbb{C}$ with $\mathbb{R}^2$ and $\zeta = x + iy$ with (x, y). We rewrite the Hamilton equations of system (1) in a compact real form as

$$\dot{\zeta} = J\nabla_\zeta H(t,\zeta)\,, \tag{6}$$

where J is the standard 2×2 symplectic matrix and $\nabla_\zeta = (\frac{\partial}{\partial x}, \frac{\partial}{\partial y})$.

The Hamilton function $H(t, \zeta)$ is piecewise autonomous and may be expressed in the form:

$$H(t,\zeta) = \phi(t)H_+(\zeta) + (1-\phi(t))H_-(\zeta)\,,$$

where

$$H_\pm(\zeta) = \frac{\Gamma}{2\pi}\ln\left|\frac{\zeta \mp b}{b\zeta \mp R^2}\right|\,, \tag{7}$$

and $\phi(t)$ is the T–periodic extension of the restriction to $[0, T]$ of the characteristic function of $[0, T/2]$. Hence, defining $\mathcal{D} := \mathbb{R}^2 \setminus \{\pm b, \pm R^2/b\}$, $H(t, \zeta)$ is smooth on the set $(\mathbb{R} \setminus \{kT/2, k \in \mathbb{Z}\}) \times \mathcal{D}$. Moreover, H and its derivatives with respect to ζ, which exist in $\mathcal{D}$ for any $t \in \mathbb{R}$, have jump discontinuities at $t = kT/2$, $k \in \mathbb{Z}$.

Next step is to consider T as a small parameter and to determine a suitable comparison limit system when $T \to 0$. For this aim, as in [1], we first rescale time in (6) by $t = T\tau$, so normalizing to 1 the period of the stirring protocol and of the vector field. In the new time τ, setting $H_1(\zeta,\tau) := H(\zeta,\tau T)$ and $y(\tau) := \zeta(\tau T)$, system (6) takes the form

$$\dot{y}(\tau) = TJ\nabla_y H_1(\tau, y)\,. \tag{8}$$

To this system the theory of averaging applies (see [6][Section 4.4]) as follows. Denote by

$$\hat{H}_1(y) := \int_0^1 H_1(\tau,y)\,d\tau \;= \frac{\Gamma}{4\pi}\ln\left|\frac{y^2-b^2}{y^2-R^4/b^2}\right| \tag{9}$$

and let $V \subset \mathbb{C}$ be an open set such that its closure is contained in D. Then for small enough $T_0 > 0$ we can find a symplectic [1], close to identity, change of coordinates of the form

$$y = \eta + Tw(\tau, \eta), \quad (\tau, \eta, T) \in \mathbb{R} \times V \times (0, T_0]\,, \tag{10}$$

with w 1–periodic in τ and such that

$$w(0, \eta) = 0\,, \tag{11}$$

which transforms system (8) into system

$$\dot{\eta} = TJ\nabla_\eta \hat{H}_1(\eta) + T^2 h(\tau, \eta, T)\,. \tag{12}$$

By construction, the function $h(\tau, \eta, T)$ in (12) is 1–periodic in τ, has jump discontinuities at $\tau = k/2$, $k \in \mathbb{Z}$ and it is smooth on $(\mathbb{R} \setminus \{k/2, k \in \mathbb{Z}\}) \times V \times [0, T_0]$.

System (8) is a perturbation of the following (integrable) *averaged system*

$$\dot{\eta} = TJ\nabla_\eta \hat{H}_1(\eta)\,. \tag{13}$$

Henceforth, for simplicity, we will write $\hat{H}$ instead of $\hat{H}_1$.

We note that the Hamilton function $\hat{H}$ corresponds to a two point vortices system, one vortex being located at $(+b, 0)$ and the second at $(-b, 0)$. Moreover, exploiting the geometry of the phase space of system (13), we can construct explicitly the action variable for this system outside the homoclinic loops surrounding the vortices (see Figure 1 on the left for $T = 0.05$). This is done as follows.

By introducing symplectic polar coordinates $\zeta = \sqrt{2r}e^{i\psi}$ and setting for notational convenience $E = e^{4\pi\hat{H}/\Gamma}$ we can express the level lines of $\hat{H}$ outside the homoclinic loops

$$r(\psi) = \frac{b^2 R^4}{R^4 + b^4} \cos 2\psi, \quad \psi \in \left[-\frac{1}{4}\pi, \frac{1}{4}\pi\right] \cup \left[\frac{3}{4}\pi, \frac{5}{4}\pi\right]\,, \tag{14}$$

in the form $r = r(\psi, E)$ with $\psi \in \mathbb{R}$ and $E \in (b^2/R^4, 1/R^2]$. We observe that $E = 1/R^2$ corresponds the boundary of D_R, whereas b^2/R^4 corresponds to the homoclinic loops.

Taking into account that $r(\psi, E) = r(-\psi, E) = r(\pi - \psi, E)$ (namely the averaged system is invariant with respect to $\zeta \to \bar{\zeta}$ and $\zeta \to -\bar{\zeta}$), the action variable I is given by

$$I(E) = \frac{1}{2\pi} \int_{\hat{H}(\sqrt{2r}e^{i\psi}) = \frac{\Gamma}{4\pi}\ln E} r\, d\psi = \frac{a(E)}{2\pi} \int_0^{\pi/2} \sqrt{b(E)\cos^2(2\psi) + c(E)}\, d\psi\,, \tag{15}$$

[1] Introducing canonical variables $y = (p, q)$ and $\eta = (P, Q)$ the requested transformation can be obtained trough the following generating function $S(q, P, \tau) = Pq + T\int_0^\tau \left[\hat{H}_1(P, q) - H_1(P, q, s)\right] ds$. Thus $p = \partial_q S$ can be inverted if T is small enough and trivially $S(q, P, \tau + 1) = S(q, P, \tau)$ for all (q, P, τ) which implies (11).

where

$$a(E) := \frac{1}{1-E^2b^4}\,, \quad b(E) := 4b^4(1-E^2R^4)^2$$
$$c(E) := 4(E^2b^4-1)(b^4-E^2R^8)\,.$$

In next proposition, we use the action variable constructed above to show that the 1–Poincaré operator of the averaged system, which henceforth we denote by $\hat{M}_1^T$, is a small twist map on an appropriate annular region inside D_R.

Proposition 1. *The set*

$$\mathcal{E} := \left\{ E \in \left(\frac{b^2}{R^4}, \frac{1}{R^2} \right] : I'(E) \neq 0 \text{ and } EI''(E) + I'(E) \neq 0 \right\},$$

is a non empty interval. Fix $E_0 \in (\inf \mathcal{E}, \frac{1}{R^2})$ and consider the annulus

$$A := \left\{ \zeta \in D_R : \frac{\Gamma}{4\pi} \ln E_0 \leq \hat{H}(\zeta) \leq \frac{\Gamma}{4\pi} \ln \frac{1}{R^2} \right\}. \tag{16}$$

Then, $\hat{M}_1^T$ is a small twist map in A.

Proof. An easy computation shows that $1/R^2 \in \mathcal{E}$. The rest of the statement about $\mathcal{E}$ follows from the continuity of the maps $E \mapsto I'(E)$, $E \mapsto EI''(E) + I'(E)$. Let us consider action–angle coordinates (θ, I) for the averaged Hamiltonian system (13), with I given by (15). In the annular domain A, defined by (16), the map $I = I(\hat{H}) := I(E(\hat{H}))$ has an inverse $\hat{H} = \hat{H}(I)$ on the interval $[I_0, R^2/2]$, where $I_0 := I(E_0)$. Moreover, on such interval we have $\hat{H}''(I) \neq 0$. Since, $\hat{H}''(1/R^2) < 0$, it follows that

$$\hat{H}''(I) < 0, \quad I \in [I_0, R^2/2]\,. \tag{17}$$

The 1–Poincaré map associated to system (13) admits a lift to the set $\mathcal{A} := \mathbb{R} \times [I_0, R^2/2]$ given by $\hat{M}_1^T(\theta, I) = (\theta + T\hat{H}'(I), I)$ and therefore, taking also into account (17), it follows that it is a small twist map. □

In order to apply Moser's Small Twist Theorem, we need some further estimates, which will be provided by the consequences of the Peano's Theorem stated below.

2.2. **Differentiability with respect to parameters.** Let $T > 0$ be the period of the stirring protocol (3) and let M_1^T be the 1–Poincaré operator of system (12). In this subsection we will recall a general result, namely Proposition 2 below, which is a consequence of the differentiability of the flow of a system of O.D.E.'s with respect to parameters. This proposition is a restatement of Proposition 6.4 in [14] under the standard assumptions considered in dealing with vector fields which are discontinuous in the independent variable. This result will provide the estimates needed to show that, for sufficiently small T, the maps M_1^T and $\hat{M}_1^T$ are C^4–close on the annulus A defined by (16).

This will be done in the next subsection, and the proof of our main result will follow easily.

Let V be an open subset of $\mathbb{R}^n$, let T_0 be a fixed positive number and let m be a nonnegative integer. Consider the following differential equation depending on one parameter

$$\frac{dx}{dt} = F(t,x,T)\,, \tag{18}$$

where $F : [0,1]\times V\times[0,T_0] \to \mathbb{R}^n$, $\quad (t,x,T) \mapsto F(t,x,T)$ is a function which satisfies

- the map $(x,T) \mapsto F(t,x,T) \in C^{m+1}(V\times[0,T_0])$ for almost all $t\in[0,1]$;
- for $0 \le j+k \le m+1$, the maps $t \mapsto \frac{\partial^{k+j}}{\partial x^k \partial T^j}F(t,x,T)$ are t measurable for any $(x,T)\in V\times[0,T_0]$;
- for each compact set $K\subset V$ there exists $C>0$ such that
$$\Big|\frac{\partial^{k+j}}{\partial x^k \partial T^j}F(t,x,T)\Big| \le C\,,$$
for all $0\le k+j\le m+1$ and $(t,x,T)\in[0,1]\times K\times[0,T_0]$.

The solution of (18) satisfying $x(0)=x_0$, will be denoted by $x(t;x_0,T)$. By the general theory of ordinary differential equations, x is of class $C^{0,m+1,m+1}$ in its three arguments whenever it is defined. The following result is a consequence of this fact.

Proposition 2. *Let A be a compact subset of V such that for every $x_0\in A$ and $T\in[0,T_0]$ the solution $x(t;x_0,T)$ is well defined in $[0,1]$. Then, for each $(t,x_0,T)\in[0,1]\times A\times[0,T_0]$ the expansion below holds*

$$x(t;x_0,T) = x(t;x_0,0) + \frac{\partial x}{\partial T}(t;x_0,0)T + R(t;x_0,T)T\,,$$

where the remainder R satisfies

$$||R(t;\cdot,T)||_{C^m(A)} \to 0, \quad T\to 0\,,$$

uniformly in $t\in[0,1]$.

2.3. **Proof of Theorem 1.** We are now able to prove our main theorem. We will show that for sufficiently small T the T–Poincaré map associated to system (1) with the stirring protocol (3) has invariant curves in the set A defined by (16).

For a fixed R' satisfying $R<R'<R^2/b$, we define

$$V := \Big\{\zeta = \sqrt{2r}e^{i\psi}\in\mathbb{C} : \frac{b^2R^4}{R^4+b^4}\cos 2\psi < r < (R')^2/2\Big\}\,. \tag{19}$$

This set, which contains A, corresponds to the open disk of radius R' minus the compact region bounded by the homoclinic loops. Hence, it has positive distance from the singularities of $\hat{H}$. Now we choose a sufficiently small $T_0>0$ for which the transformation (10) is well defined on $[0,1]\times V\times[0,T_0]$ and, moreover, all the solutions of system

(8) with initial conditions in A are well defined in $[0,1]$. Let $T < T_0$ be the period of $z(t)$. By Proposition 2, and by introducing the action angle coordinates considered in Proposition 1, we can find a lift of M_1^T to $\mathcal{A} := \mathbb{R} \times [I_0, R^2/2]$ of the form

$$M_1^T(\theta, I) = (\theta + \hat{H}'(I)T, I) + R(\theta, I, T)T\,,$$

where $||R(\cdot, T)||_{C^4(\mathcal{A})} \to 0$ for $T \to 0$. Hence, M_1^T satisfies hypothesis b) of Moser's Small Twist Theorem for T small enough. Moreover, M_1^T has the intersection property in A, being an area–preserving map in A for which the boundary of A is invariant.

Then, by Moser's Small Twist Theorem, M_1^T has many invariant curves in A for T small enough, and so does the T–Poincaré operator of system (1), which obviously coincide with M_1^T.

3. Numerical Results

In this section we will study system (1) with the stirring protocol (3) from a numerical point of view. More precisely, we will be interested in two types of numerical experiments. In the first one, we will explore the *continuation* properties with respect to T of the invariant curves of the T–Poincaré map of system (1) obtained for small T in Theorem 1. In §3.2, we will give numerical evidence of their persistence close to the boundary for large values of T.

In the second experiment, we will be able to give a *quantitative* description of the mixing efficiency of the piecewise constant stirring protocol. This will be done in §3.3, where we will investigate the parameters (b, T) giving rise to an efficient stirring.

Both these numerical experiments will be carried out by using the *Numerical Analysis of the Fundamental Frequency (NAFF)* of Laskar[10].

This is a numerical method which allows to obtain a global view of the behavior of a dynamical system by studying the properties of the frequency map, numerically defined from the action–like variables to the frequency space using adapted Fourier techniques. This method has been used to investigate a wide class of dynamical systems, such as the solar system [11], the galactic dynamics [15], particle accelerators [12] and the standard map [3].

For sake of completeness, let us first present briefly the main outlines of the method, referring to [10] for further details.

3.1. Frequency Map Analysis.

Let us consider an n–degrees of freedom quasi–integrable Hamiltonian system, expressed in action–angle variables by

$$H(I, \theta; \epsilon) = H_0(I) + \epsilon H_1(I, \theta)\,, \tag{20}$$

where H is a real analytic function of $(I, \theta) \in B \times \mathbb{T}^n$, B is an open domain in $\mathbb{R}^n$, $\mathbb{T}^n$ is the n–dimensional torus and ϵ is a small real parameter. For $\epsilon = 0$ the system is integrable: the motion takes place on invariant tori $I_j = I_j(0)$ described at constant velocity $\nu_j(I) = \left.\frac{\partial H_0}{\partial I_j}\right|_{I(0)}$, for $j = 1, \ldots, n$. Assuming a non–degeneration condition on H_0, the frequency map $F : B \to \mathbb{R}^n$

$$F : I \mapsto F(I) = \nu\,,$$

is a diffeomorphism onto its image Ω. In this case KAM theory [9, 2, 13] ensures that for sufficiently small values of $|\epsilon|$, there exists a Cantor set $\Omega_\epsilon \subset \Omega$ of frequency vectors satisfying a Diophantine condition, for which the quasi–integrable system with Hamilton function (20) still possess smooth invariant tori. These tori are ϵ–close to those of the unperturbed system, and support the linear flow $t \mapsto \theta_j(t) = \nu_j t + \theta_j(0) \pmod{2\pi}$ for $j = 1, \ldots, n$. Moreover, according to Pöschel [16] there exists a diffeomorphism $\Psi : \mathbb{T}^n \times \Omega \to \mathbb{T}^n \times B$

$$\Psi : (\phi, \nu) \mapsto (\theta, I)\,,$$

which is analytic with respect to ϕ in $\mathbb{T}^n$ and $\mathcal{C}^\infty$ w.r.t ν in Ω_ϵ, and which transforms the Hamiltonian system generated by (20) into

$$\begin{cases} \frac{d\nu_j}{dt}(t) = 0 \\ \frac{d\phi_j}{dt}(t) = \nu_j\,. \end{cases}$$

For frequency vectors $\nu \in \Omega_\epsilon$, the invariant torus can be represented in the complex variables $(z_j = I_j e^{i\theta_j})_{j=1,n}$ by a quasi–periodic function

$$z_j(t) = z_j(0)\, e^{i\nu_j t} + \sum_m a_{j,m}(\nu)\, e^{i<m,\nu>t}\,. \tag{21}$$

Taking a section $\theta = \theta_0$ of the phase space, for some $\theta_0 \in \mathbb{T}^n$, we obtain the frequency map $F_{\theta_0} : B \to \Omega$

$$F_{\theta_0} : I \mapsto \pi_2\left(\Psi^{-1}(\theta_0, I)\right)\,, \tag{22}$$

where $\pi_2(\phi, \nu) = \nu$ is the projection onto Ω. For sufficiently small $|\epsilon|$ the non–degeneration condition ensures that F_{θ_0} is a smooth diffeomorphism.

If we have a numerical (complex) signal over a finite time span $[-K, K]$ and we want to recover a quasi–periodic structure, we can construct an N–terms quasi–periodic approximation $\hat{f}(t) = \sum_{k=1}^N a_k^{(K)} e^{it\nu_k^{(K)}}$. Frequencies $\nu_k^{(K)}$ and amplitudes $a_k^{(K)}$ are determined with an iterative scheme (possibly) involving some weight function (Hanning filter).

Assuming some "good" arithmetic properties of the frequencies and using the p–th Hanning filter, then one can prove [10] that NAFF converges towards the first[2] "true" frequency of the given signal, ν_1,

[2]We assume to enumerate frequencies according to decreasing amplitudes: $|a_k^{(K)}| \geq |a_{k+1}^{(K)}|$. That is, some smoothness of the signal is assumed.

with the following asymptotic expression for $K \to +\infty$

$$|\nu_1 - \nu_1^{(K)}| = \mathcal{O}\left(\frac{1}{K^{2p+2}}\right) , \tag{23}$$

which will usually be several order of magnitude better than the $\mathcal{O}(1/K)$ order obtained with FFT.

Using the NAFF algorithm, it is possible to construct numerically a frequency map (see Figure 2) in the following way:

a) fix all angles to some value θ_0;
b) for all initial values I_0 of the action variables, integrate numerically the trajectories with initial condition (I_0, θ_0) over the time span K;
c) look for a quasi–periodic approximation of the trajectory, with the previous algorithm identifying the fundamental frequency $\nu_1^{(K)}$ of this quasi–periodic approximation.

Because of (23), we can use NAFF algorithm to test the goodness of the reconstructed quasi–periodic approximation of the given signal, showing numerical evidence that motion doesn't take place on invariant tori because of some "diffusion in frequency space". More precisely, this can be done by replacing step c) of the previous algorithm with the following

c') divide the time span $[-K, K]$ into smaller parts (possibly overlapping): $[t_l, t_l + K_1]$, for some t_l. Then NAFF reconstructs for each l a frequency $\nu^{(K_1)}(l)$. If the frequencies $(\nu^{(K_1)}(l))_l$ coincide, up to some prescribed numerical precision, when l varies, then we can conclude that we obtained a good quasi–periodic approximation. Otherwise, we can measure the diffusion in the frequency space.

3.2. **Application I: existence of invariant curves.** Let us consider the problem of the existence of invariant curves homotopic to the boundary of D_R for the T–Poincaré map of system (1) with stirring protocol (3). One readily realizes that every such curve will intersect the vertical segment $\ell := \{\zeta \in \mathbb{C} : x = 0\,,\, y \in [0, R]\}$.

In order to reconstruct a frequency map, we fix a piecewise constant stirring protocol by choosing the parameters (b, T). Then, for N initial data on the segment ℓ we construct numerically the T–Poincaré map and we iterate it N_{iter} times.

Remark 1 (Numerical computation of the Poincaré map). *As already remarked in* [1], *one can construct the Poincaré map for the piecewise constant protocol avoiding the integration of the Hamiltonian system (1), which results CPU–time consuming and introduces additional errors. The idea is that in each half period the Hamiltonian system is autonomous, hence integrable and, moreover, the integration can be explicitly done: for* $t \in [0, T/2)$, *the motion takes place on an arc of* *circle with radius* $\rho = \frac{\lambda}{1-\lambda^2}\left(\frac{R^2}{b} - b\right)$*, centered at* $\zeta_c = \frac{b^2-\lambda^2 R^2}{b(1-\lambda^2)}$*, with* $\lambda = b\left|\frac{\zeta(0)-b}{b\zeta(0)-R^2}\right|$*. Thus, setting* $\zeta(0) = \zeta_c + \rho e^{i\phi(0)}$*, after half period the point will be at* $\zeta(T/2) = \zeta_c + \rho e^{i\phi(T/2)}$ *where:*

$$\phi(T/2) - \frac{2\lambda}{1+\lambda^2}\sin\phi(T/2) = \frac{\Gamma}{2\pi\rho^2}\frac{1-\lambda^2}{1+\lambda^2}\frac{T}{2}\,. \tag{24}$$

The motion in the second half period is similar.

Equation (24) can be solved using a sixth order Newton's–type method. However, when b *is close to* R *and/or* T *is large, Newton's algorithm doesn't converge to the good solution unless we provide a very accurate approximation of* $\phi(T/2)$ *as initial value for the algorithm. In order to overcome this difficulty, we used the following trick. Equation (24) is nothing but* Kepler's equation *and in* [17] *an explicit solution is given in terms of Bessel's functions (which results, in computations, less efficient than our Newton's–type method). Neverthless for large values of the parameters we obtain a good approximation to start with Newton's algorithm by summing few terms of the previous explicit solution.*

Once we have an orbit, $\left(M_T^k(\zeta(0))\right)_{0\le k\le N_{iter}}$, we use the NAFF algorithm to reconstruct a quasi–periodic approximation of it. The frequency map is not smooth at all because of the presence of resonances: there is no invariant curve with rational rotation number. Thus, for a fixed resolution, the existence of invariant curves is assumed if the frequency map looks "regular" (see Figure 2 for $T = 0.05$), whereas to "irregular" graphs we associate non existence of invariant curves (see Figure 3 for $T \in \{0.5, 1.0, 1.5\}$).

In Figure 2 we present some numerical results for the piecewise constant protocol (3) with $b = 1/2$ and several values of T. On the left, for very small T, say 0.05, the curve looks regular, hence a large part of the disk is occupied by invariant curves. We can observe that the map *is not twist* in the whole disk: there is a point where the derivative of the frequency map is zero. For slightly larger T, say $T \in (0.125, 0.2)$, the curve is still regular, but an irregular pattern is showed close to the origin. Roughly speaking, no invariant curves are present for $T = 0.2$ in the disk $|\zeta| \le 0.22$. Also, elliptic points due to resonances are showed.

In Figure 3, when T increases, the irregular patterns consume larger and larger portions of the invariant disk, but still a regular frequency map is present close to the boundary of D_R.

This behavior of the system is displayed in Figure 4, where we show a numerical result for $b = 1/2$ and $T = 3.0$, a period which is 60 times larger than the smallest value in Figure 2. Note the change in the scale on the axes w.r.t. to Figure 2 and 3 (the scale on the vertical axis has been changed to show the large oscillations of the frequency map).

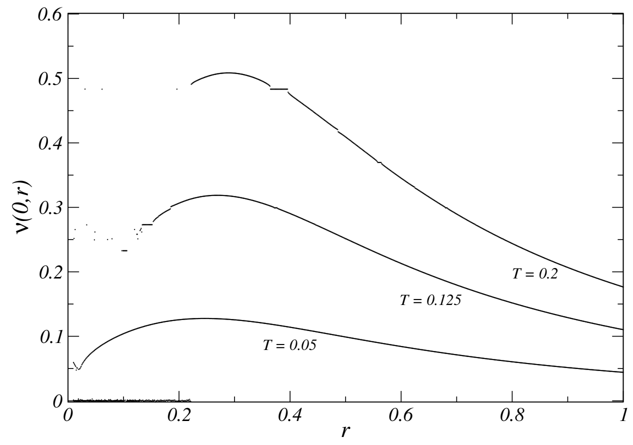

FIGURE 2. The Frequency Map numerically reconstructed by NAFF. Parameters are $b = 1/2$, $R = 1$ and $T \in \{0.05, 0.125, 0.2\}$. Initial data are 1000 points $\zeta_j(0) = ir_j$, equally spaced on $[0, i]$ and orbits are comput

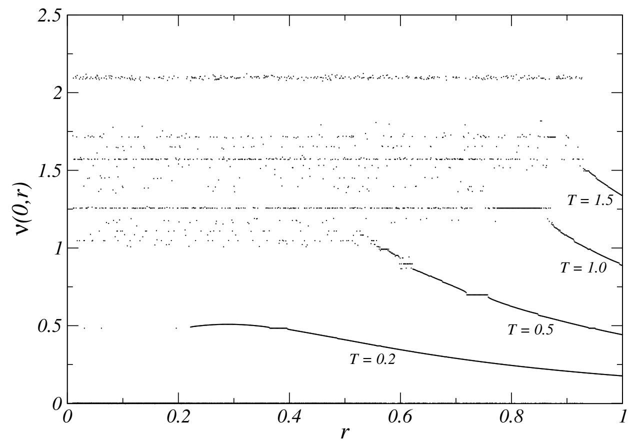

FIGURE 3. The Frequency Map numerically reconstructed by NAFF. Parameters are $b = 1/2$, $R = 1$ and $T \in \{0.2, 0.5, 1.0, 1.5\}$. Initial data are 1000 points $\zeta_j(0) = ir_j$, equally spaced on $[0, i]$ and orbits are computed for $N_{iter} = 50000$.

Other results for larger values of T exhibit a similar behavior. This supports the conjecture that invariant curves persist, close to the boundary, for arbitrarily large values of T.

3.3. **Application II: mixing efficiency.** We have already observed that invariant curves are an obstruction to global mixing. We note now that close to *robust* invariant curves (i.e. associate to good frequencies) there is a neighborhood filled by invariant curves [4, 5], which prevents

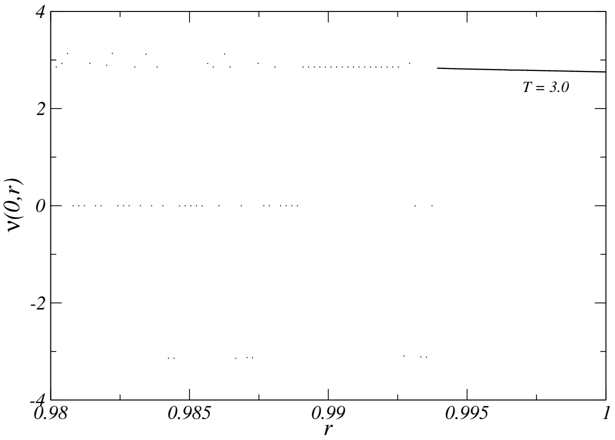

FIGURE 4. The Frequency Map numerically reconstructed by NAFF. Parameters are $b = 1/2$, $R = 1$ and $T = 3.0$. Initial data are 1000 points $\zeta_j(0) = ir_j$, equally spaced on $[0.98i, i]$ and orbits are computed for $N_{iter} = 500000$.

also from local mixing. Using the precision of NAFF and observation c') in page 10, we can test the efficiency of the stirring protocol by evaluating the goodness of the reconstructed signal.

More precisely, we choose a couple of parameters (b, T), then we divide the invariant disk D_R into a fine grid of N_{tot} points. For each point we determine numerically (see Remark 1) the orbit for a time interval $[0, K]$. Then, fixing some $K_1 < K$ and some positive $(t_l)_l$ we divide the orbit into pieces $(\zeta(t))_{t\in[t_l,t_l+K_1]}$ such that intervals $[t_l, t_l+K_1]$ overlap. On each piece, the use of NAFF gives us a fundamental frequency $\nu^{(K_1)}(l)$, where we emphasize the dependence of the frequency on the l–piece of orbit.

For a given orbit with initial datum $\zeta_0 = (x_0, y_0)$, let us define

$$\varepsilon(x_0, y_0) = -\log\left|2\frac{\max_l \nu^{(K_1)}(l) - \min_l \nu^{(K_1)}(l)}{\max_l \nu^{(K_1)}(l) + \min_l \nu^{(K_1)}(l)}\right|. \tag{25}$$

This is a good indicator of the robustness of the orbit. In fact, if $\varepsilon(x_0, y_0)$ is "large" then $\max_l \nu^{(K_1)}(l)$ and $\min_l \nu^{(K_1)}(l)$ are "close together". Thus, the reconstructed frequencies on different pieces of orbit do not vary too much, and we can assume that we are on a quasi–periodic orbit. On the other hand, if $\varepsilon(x_0, y_0)$ is "small" then $\max_l \nu^{(K_1)}(l)$ and $\min_l \nu^{(K_1)}(l)$ are "far from each other". In this case, since the reconstructed frequency is not constant, we conclude that we are not on a quasi–periodic orbit. Intermediate values of $\varepsilon(x_0, y_0)$ give rise to intermediate degrees of robustness.

We now fix a threshold value $\varepsilon_{thr} > 0$ and we measure the portion of initial data in D_R to which one can associate a ε_{thr}–robust orbit

$$m_{\varepsilon_{thr}} = \frac{\#\{(x_0, y_0) : \varepsilon(x_0, y_0) > \varepsilon_{thr}\}}{\#\{(x_0, y_0)\}} . \tag{26}$$

A preliminary analysis, see Figure 5, of some robust orbits allows us to choose an appropriate threshold value.

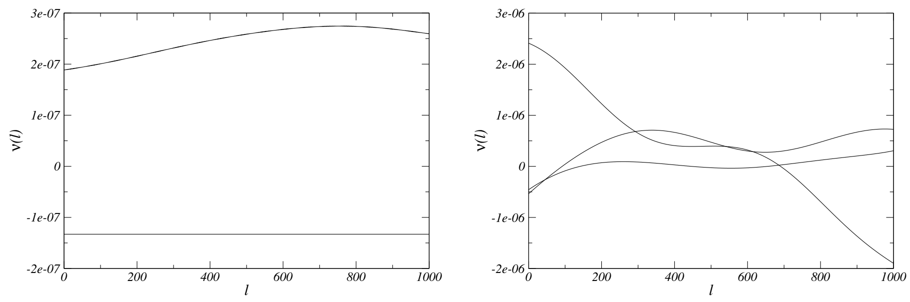

FIGURE 5. Distance between the frequency $\nu_1^{(K_1)}(l)$, determined by NAFF, and the mean value of the $\nu_1^{(K_1)}(l)$'s, in function of the part of orbit $[t_l, t_l + K_1]$. On the left very regular orbits, on the right less regular ones. Both plots are made with $N_{iter} = 100000$, $K_1 = 50000$ and $t_l = 50(l-1)$.

In this way we are able to turn the *qualitative* analysis of Figure 7 page 738 of [1] into a *quantitative* one.

With this respect, we present two results, the first with $\varepsilon_{thr} = 12$, corresponding to $\left|\frac{\max_l \nu^{(T_1)}(l)}{\min_l \nu^{(T_1)}(l)} - 1\right| \leq 3\,10^{-6}$, and the second with $\varepsilon_{thr} = 15$ and $\left|\frac{\max_l \nu^{(T_1)}(l)}{\min_l \nu^{(T_1)}(l)} - 1\right| \leq 1.5\,10^{-7}$. Each result has been obtained dividing the invariant disk in approximately 30000 points, equally spaced in both x and y by 0.01. Then, several values of b and T have been considered.

Finally, by using the previous ideas, we precise as follows the classification scheme given for a regime in [1]:

[I] *integrable* if $0.6 < m_{\varepsilon_{thr}} \leq 1$ (very poor mixing property) ;
[T] *transitional* if $0.3 < m_{\varepsilon_{thr}} \leq 0.6$;
[C] *chaotic* if $0 < m_{\varepsilon_{thr}} \leq 0.3$ (efficient mixing),

and we summarize our results in the following Figure 6

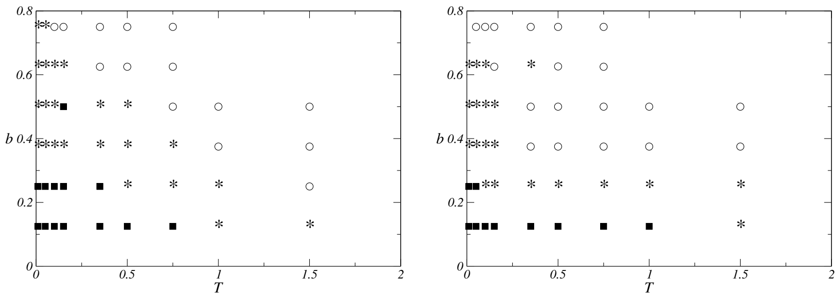

FIGURE 6. A part of parameter plane and the corresponding $m_{\varepsilon_{thr}}$ function; on the left m_{12}, on the right m_{15}. Squares correspond to Integrable case, stars to Transitional whereas circles to chaotic.

4. CONCLUSIONS

In this paper we proved that the simple stirring model given by (1) has invariant curves for all T small enough and every $b \in (0, R)$; the use of NAFF gives us numerical evidence that such invariant curves persists even for T large, closer and closer to the boundary of the disk as T increases. Hence, for small T the mixing efficiency in not good at all, whereas for larger values of T, say $T > 1$, it becomes reasonably good once $b \geq R/2$. Thus, even if very simple, the model can give rise to efficient mixing.

We note that, due to the general results on which it relies, our proof of the existence of invariant curves for small T may work for more general T–periodic stirring protocols $z(t)$. However, the starting point should be to obtain a 'simple' averaged system.

From the numerical point of view, the more general systems referred above can be surely studied by means of NAFF method, once we obtained good integrators for these systems. Still considering our piecewise constant model, we think that using NAFF one could give precise estimates of the size of the annular domain close to the boundary of D_R containing invariant curves and of the rate at which it shrinks to zero when T increases to infinity.

REFERENCES

[1] H. AREF: Stirring by chaotic advection, *J. Fluid Mechanics*, **143** (1984), pp. 725–745.

[2] V.I. ARNOLD: Proof of a Theorem of A.N. Kolmogorov on the invariance of quasiperiodic motions under small perturbations of the Hamiltonian, *Usp. Mat. Nauk.*, **18** 13, (1963); *Russ. Math. Surv.*, **18**, (1963), pp. 9–36.

[3] T. CARLETTI AND J. LASKAR: Scaling law in the standard map critical function, Interpolating Hamiltonian and frequency analysis, *Nonlinearity*, **13**, (2000), pp. 1-29.

[4] A. GIORGILLI AND A. MORBIDELLI: Superexponential stability of KAM tori, *J. Statist. Phys.*, **78**, no. 5-6, (1995), pp. 1607–1617.

[5] A. Giorgilli and A. Morbidelli: On a connection between KAM and Nekhoroshev's theorems, *Phys. D*, **86**, no. 3, (1995), pp. 514–516.

[6] J. Guckenheimer and P. Holmes: Nonlinear oscillations, Dynamical Systems, and Bifurcation of Vector Fields, *Applied Math. Sciences,* **42** Springer Verlag (1983).

[7] M.R. Herman: Sur les courbes invariantes par les difféomorphismes de l'anneau I, *Asterisque I*, $\mathbf{103-104}$, (1983).

[8] M.R. Herman: Sur les courbes invariantes par les difféomorphismes de l'anneau I, *Asterisque II*, **144**, (1986).

[9] A.N. Kolmogorov: Preservation of conditionally periodic movements with small change in the Hamilton function, *Dokl. Akad. Nauk SSSR*, **98**, (1954), pp. 527–530.

[10] J.Laskar: Introduction to Frequency Map Analysis, *In the proceedings of 3DHAM95 NATO Advanced Institute* 533*, S'Agaro, June 1995*, (1999), pp. 134–150.

[11] J.Laskar: The chaotic motion of the solar system. A numerical estimate of the size of the chaotic zones, *Icarus* **88**, (1990, pp. 266–291.

[12] J.Laskar and D.Robin: Application of frequency map analysis to the ALS, *Particle Accelerator*, **54**, (1996), pp. 183–192.

[13] J.K.Moser: On invariant curves of area preserving mappings of an annulus, *Nachr. Akad: Wiss. Gottingen Math. Phys. II*, (1962), pp. 1–20.

[14] R. Ortega: Twist Mappings, Invariant Curves and Periodic Differential Equations, *Progress in Nonlinear differential Equations and Their Applications*, **43** Birkhauser, (2000).

[15] Papaphilippou, Y., Laskar, J.: Frequency map analysis and global dynamics in a two degrees of freedom galactic potential, *Astron. Astrophys.*, **307**, (1996), pp. 427–449.

[16] J.Pöschel: Integrability of Hamiltonian systems on Cantor sets, *Comm.Pure Appl.Math.*, **25**, (1982), pp. 653–695.

[17] G.N. Watson: A treatise on the Theory of Bessel functions, second edition, Cambridge University Press, (1966).

(T. Carletti) Scuola Normale Superiore, piazza dei Cavalieri, 7, 56126 Pisa, Italy

(A. Margheri) Fac. Ciências de Lisboa and Centro de Matemática e Aplicações Fundamentais, Av. Prof. Gama Pinto 2, 1649-003 Lisboa, Portugal

E-mail address, Timoteo Carletti: `t.carletti@sns.it`

E-mail address, Alessandro Margheri: `margheri@ptmat.fc.ul.pt`